

computationally with the typically large data sets involved. An ideal computational visualization environment would permit access to the greyscale data while having a transparent volume to interactively move on arbitrary as well as orthogonal axes, and incorporate 3D measurement tools. While freeware volume visualization packages are available, currently each falls short in some aspect. Our laboratory currently uses the commercial package, Amira (www.tgs.com).

National Resources available in the United States.

Boulder Laboratory for 3-Dimensional Fine Structure Tomography	bio3d.Colorado.edu
National Center for Microscopy and Imaging Research Tomography	www.ncmir.ucsd.edu
National Center for Macromolecular Imaging SPR	ncmi.bcm.tmc.edu/ncmi
Resource for Visualization of Biological Complexity	www.wadsworth.org/rvbc

[4] Electron Microscopic Analysis of the RSC Chromatin Remodeling Complex

By FRANCISCO J. ASTURIAS, CHUKWUDI EZEOKONKWO,
ROGER D. KORNBERG, and YAHLI LORCH

Introduction: Use of Electron Microscopy for Analysis of Large Macromolecular Complexes

Macromolecular electron microscopy (EM) is an ideal technique for structural characterization of large (>300,000 Da) macromolecular complexes, which may be too difficult to purify to homogeneity in the large quantities required for more conventional techniques, such as X-ray crystallography. Single-molecule-thick 2D crystals suitable for EM crystallographic analysis can be prepared using the lipid layer crystallization technique,^{1,2} which requires two to three orders of magnitude less material (typically 10–100 μg of protein) than would be required for preparation of 3D crystals. Even smaller amounts of material (1–5 μg) are required for the preparation of samples from which single-particle images can be obtained

¹ F. J. Asturias and R. D. Kornberg, *J. Biol. Chem.* **274**, 6813 (1999).

² E. E. Uzgiris and R. D. Kornberg, *Nature* **301**, 125 (1983).

and later analyzed to generate structures at a resolution of 10–30 Å.³ We have used single-particle image analysis techniques to characterize the structure of RSC, an abundant, essential chromatin remodeling complex from the yeast, *Saccharomyces cerevisiae*.⁴ A 3D reconstruction of RSC obtained from images of negatively stained particles suggests a possible mode of interaction between the complex and a nucleosome core particle.

Sample Preparation for Electron Microscopy of Single Particles Preserved in Stain

Preservation in a heavy metal stain offers a quick and simple method to preserve biological macromolecules for imaging in the electron microscope. A widely used stain is uranyl acetate, which works well with many molecular complexes. The electron-dense stain is excluded from the volume occupied by the specimen, and what is actually recorded is therefore an imprint of the macromolecule in the stain. The advantages of using a heavy metal salt stain are the ease and speed of specimen preparation and imaging. However, the specimen is visualized only indirectly and at low resolution, and in most cases is partially deformed as a consequence of dehydration and interaction with the substrate to which the macromolecules are adsorbed. Despite its shortcomings, preservation in stain is the best alternative for initial characterization of a macromolecule, and can provide useful structural information. In addition, a structure calculated from specimens preserved in stain can in many instances be used as a starting point for more precise structural characterization based on images of unstained specimens preserved in amorphous ice.

Specimens are typically prepared using carbon-coated grids. To prepare the grids, a thin (~10 nm) layer of amorphous carbon is evaporated onto a freshly cleaved mica surface. The carbon layer is released by slowly pushing the carbon-coated mica, carbon-coated side facing upward, at an angle (~45°) through an air-water interface. The grids to be carbon coated are previously arranged on a support below the water surface. After release from the mica, the carbon film is carefully manipulated to position it on top of the grids, and is deposited on them by slowly lowering the water level until the carbon film comes into contact with the grids.

³ J. Frank, “Three-Dimensional Electron Microscopy of Macromolecular Assemblies.” Academic Press, San Diego (1996).

⁴ F. J. Asturias, W. H. Chung, R. D. Kornberg, and Y. Lorch, *Proc. Natl. Acad. Sci. USA* **99**, 13477 (2002).

Specimens are prepared using a protein solution in a low-salt (<100 mM) buffer, as the presence of high-salt concentration would interfere with staining and create problems for adequate imaging of the specimen. A protein solution with a concentration in the range of 10–100 μg protein/ml usually results in an adequate density of particles in the samples. To facilitate adsorption of the molecules to the carbon support film the grids are glow-discharged at a residual pressure of $\sim 2 \times 10^{-1}$ mbar for 30–60 s. The nature of the gas used during glow discharge (air, water vapor, and amyl amine are typical choices) can be varied to affect the properties of the carbon film after glow discharge. Two to three microliters of the protein solution are placed on the surface of a freshly glow-discharged grid (the effect of glow discharge on the carbon surface only lasts for a few minutes), which is held using microforceps. The protein solution is left on the grid for 10–60 s to give the particles a chance to adsorb onto the support film, and then blotted away by touching the side of the grid to a piece of filter paper. The grid is then washed with two to three drops of 1–2% uranyl acetate. The final drop of stain is left on the grid for 30–60 s to ensure proper staining of the sample. The sample preparation process is completed by depositing a second carbon layer on top of the stained molecules. This is accomplished by floating a small piece ($\sim 5 \times 5$ mm) of carbon on the surface of a pool (~ 5 ml) of stain using the same procedure employed to release the carbon film used to coat the grids. The stained sample is then immersed in the stain pool and withdrawn through the interface to pick up the second carbon layer.^{5,6} Excess stain is removed by bringing a piece of filter paper into contact with the backside of the grid.

Preliminary Specimen Evaluation and Data Collection

While specimens preserved in negative stain are relatively resistant to radiation damage, it is nonetheless important to minimize the electron dose received by the specimen prior to imaging. Initial evaluation of the specimens entails examining the grids at low ($\sim 2000\times$) magnification. If the concentration of the protein solution used to prepare the specimens was adequate, properly stained specimens will have a “grainy” appearance, and examination at higher magnification ($\sim 35,000\times$) will reveal nicely stained particles. Properly stained particles should be clearly distinguishable from the background and show internal detail. If the amount of protein adsorbed on the carbon support surface was too low, very little stain

⁵ G. W. Tischendorf, H. Zeichhardt, and G. Stoffler, *Mol. Gen. Genet.* **134**, 187 (1974).

⁶ G. Stoffler and M. Stoffler-Meilicke, in “Modern Methods in Protein Chemistry” (H. Tesche, ed.), p. 409. De Gruyter, Berlin (1983).

will be retained and the specimen will resemble a clean carbon film. Finally, an excessive amount of material adsorbed to the carbon support film will result in samples where staining is evident, but no individual particles can be distinguished when an area is examined at higher (e.g., 35,000 \times) magnification. After determining that the staining and protein concentration in the samples are adequate, the next step is to collect images to evaluate the preservation of the particles and the distribution of particle orientations in the samples. Since individual particles must be selected for image analysis, it is important to optimize their distribution by carefully adjusting the protein concentration used during sample preparation. Ideally, particles should be evenly distributed on the support film, and the separation between individual particles should correspond to 2–3 particle diameters. This will result in a large number of particles being included in recorded images, while ensuring that it will be possible to select individual particles without interference from neighboring ones.

Most of the data for single particle analysis are still collected on film, but the use of electronic detectors is increasing, and the trend will undoubtedly continue. The arguments that follow apply to either type of data, as the distinction between them largely disappears after film data has been digitized. Zero-tilt images of the specimens are necessary to assess particle preservation and orientation. Images for data analysis are typically recorded at magnifications in the range 35,000–65,000 \times . In the case of film data, the images should be scanned using a pixel size equivalent to about one fourth of the desired resolution. The number of pixels available for alignment of individual particle images is often the more critical parameter for determining how images should be digitized.

Analysis and Classification of 2D images

The RSC images used in this study were collected at a magnification of 60,000 \times , and scanned using a pixel size corresponding to 2.54 Å in the specimen. Once the images were digitized, individual particles were cut out using a window size such that the side of the window corresponded roughly to twice the largest dimension of an RSC particle. Reference-free alignment of the particle images followed by multivariate statistical analysis and hierarchical ascendant classification³ provides information about the distribution of particle orientations, and about potential variability in particle conformation. RSC particles were found to occur mostly on a single preferred orientation, but to display a significant amount of variability in conformation. At low resolution and in projection, the RSC particle appears as formed by four globular domains arranged around a central cavity. The results of multivariate statistical analysis and hierarchical

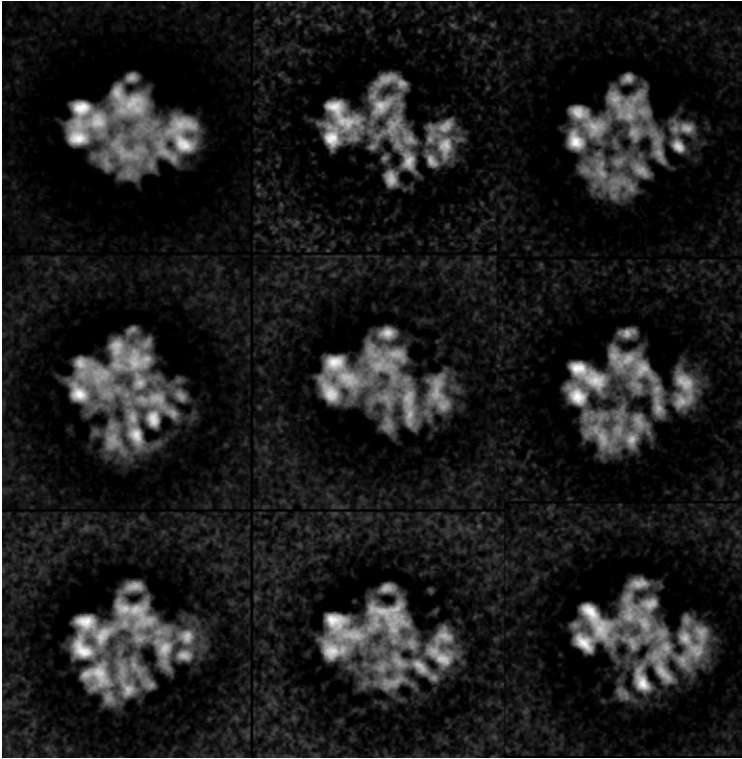


FIG. 1. Structure of RSC in projection. Images of RSC particles (5880) preserved in uranyl acetate were computationally aligned. All particles seemed to be in a similar orientation but differed in conformation and were sorted into homogeneous classes using multivariate statistical analysis and hierarchical ascendant classification.³ A central area of lower density is apparent in several of the class averages shown, which include ~45% of all particles. Most of the variation in RSC conformation is related to a domain forming the bottom part of the structure, which is either missing (~35% of particles), or collapsed against the top of the structure (~22% of particles).

ascendant classification of RSC particle images are shown in Fig. 1. While three of the four domains remain fairly constant in their relative arrangement and orientation, the fourth one (forming the lower part of the RSC structure as shown in Fig. 1) varies in position, and in some instances appears to be either absent or collapsed against the top part of the RSC structure. Given the large degree of variability shown by the RSC particles, 3D reconstructions were calculated for homogeneous subsets of particles defined by the hierarchical ascendant classification analysis.

Calculation of Initial 3-D Reconstructions

From a set of particles that correspond to a single conformation and a single orientation, an initial 3-D reconstruction can be easily calculated using the random conical tilt method,^{7,8} which is implemented by combining information from untilted and tilted images of the same specimen area. Briefly, particles in a given orientation are selected from the untilted images, along with their corresponding tilted pairs. In-plane rotational alignment parameters for the untilted particle images, the tilt angle for the corresponding tilted particle images, and information about the relative orientation between the tilted and untilted images in a tilt pair are used to calculate a 3D structure from the tilted particle images. If additional homogeneous (same conformation and orientation) particle sets can be identified, the procedure is repeated. The resulting reconstructions are then combined to make up for the incomplete information in each individual reconstruction resulting from physical limitations in the maximum value of the tilt angle used for data collection (missing cone problem).

We were able to calculate several reconstructions of the RSC complex from homogeneous particle subsets identified by statistical analysis. Some of those reconstructions are shown in Fig. 2. Comparison of the structures confirms that the differences among them arise mostly from rearrangement of a domain in the lower part of the structure that moves as a solid module. The structures could not be combined because they correspond to different conformations of the RSC complex. An additional limitation of the reconstructions relates to particle deformation induced by preservation in stain. This phenomenon is known to be significant, as surface tension forces and dehydration cause particles preserved in stain to be flattened along the direction perpendicular to the carbon support surface. The problem can be corrected when information from different views can be combined to calculate an improved reconstruction (different reconstructions are deformed in different directions and the effect of such deformation is alleviated in the final combined volume), but the presence of different conformations and a single predominant orientation prevented us from using that approach to improve the quality of the RSC reconstruction.

Interpretation of the RSC Reconstruction

As explained earlier, examination of the different 3D reconstructions of the RSC complex shown in Fig. 2 led us to conclude that the variability observed was most likely related to a change in the position of the domain

⁷ M. Radermacher, *J. Electron Microsc. Tech.* **9**, 359 (1988).

⁸ M. Radermacher, T. Wagenknecht, A. Verschoor, and J. Frank, *J. Microsc.* **146**, 113 (1987).

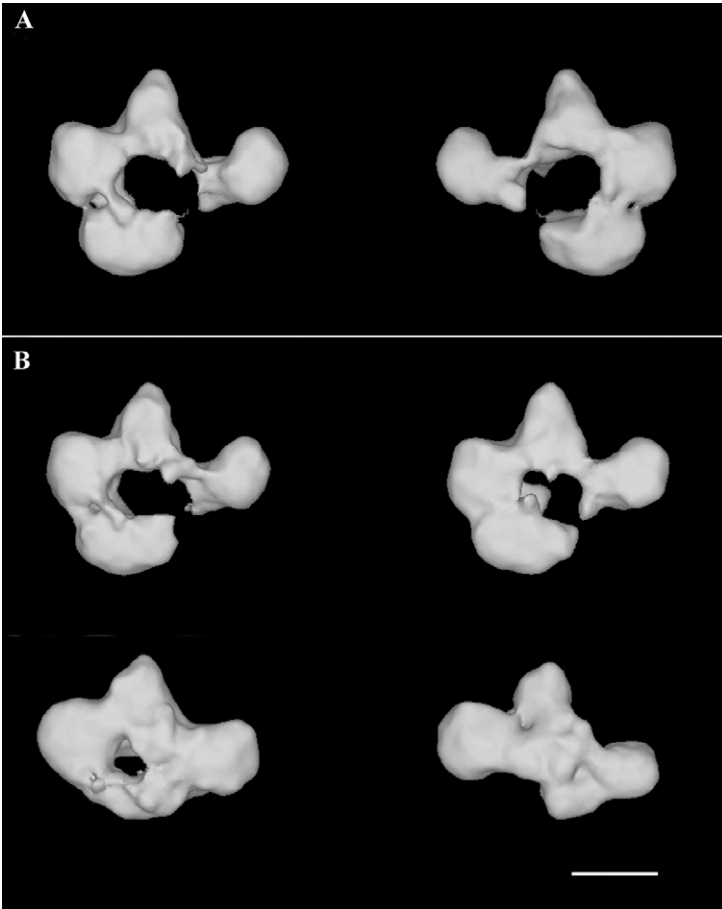


FIG. 2. Three-dimensional reconstruction of RSC. (A) RSC consists of four modules that define a central cavity. Two views of the structure (front and back) are shown. (B) The most significant variation in RSC conformation was due to the collapse (top) or absence (bottom) of a module that forms the lower part of the RSC structure. The scale bar corresponds to approximately 100 Å.

that defines the bottom portion of the central cavity. This domain seems to partially collapse under the sample preservation conditions used in the study. However, a majority of the RSC particles (~45%) show a clearly defined cavity, and that appears to be the most representative conformation of the complex. Variability in the position of the lower domain may actually have functional significance, as it could control access to the central cavity, which would be more accessible when the bottom domain moves

away from the rest of the structure. The shape and size of the central cavity in the RSC complex matches closely the shape and size of a nucleosome core particle. Possible binding of a nucleosome in the cavity was tested by calculating a reconstruction of the RSC/nucleosome complex.

Studying the RSC/Nucleosome Interaction Under EM Sample Preparation Conditions

Determining the structure of a complex formed by RSC and the nucleosome core particle (histone core plus ~ 150 pb of double-stranded DNA) would likely help to determine the mechanism by which RSC alters the interaction between the histone core and nucleosomal DNA and renders the nucleic acid more accessible to components of the transcription apparatus. RSC interacts with the nucleosome core particle with very high affinity ($K_d \sim 10^9$), and therefore formation of the complex for examination by electron microscopy should be a straightforward matter. A rough method for quantitating formation of the RSC/nucleosome complex under the conditions required for sample preparation was implemented as follows.

First, samples of RSC alone were prepared, using a protein concentration that resulted in an adequate particle density. Under the same conditions (same grids, same buffer conditions), samples of nucleosomes alone were prepared, using a nucleosome concentration that resulted in a density of nucleosome particles similar to that of the RSC particles. Once both types of samples had been prepared, the number of particles in an arbitrary area (the area corresponding to a frame collected with an electronic CCD camera detector at $66,000\times$ magnification) was determined for both the RSC and nucleosome samples. Having determined such numbers and checked that the desired ratio of RSC/nucleosome particles had been obtained, samples containing both RSC and nucleosomes were prepared in such a way that the final concentration of both RSC and nucleosomes in the solution used to prepare the mixed samples (as well as the buffer conditions, etc.) were identical to those previously used to prepare samples of the individual components. The RSC/nucleosome samples were then examined in the microscope, and the number of RSC and nucleosomes in the previously specified unit area were determined. A decrease in the number of nucleosomes with respect to that observed in the nucleosome (no RSC) samples could be considered as indirect evidence for formation of the RSC/nucleosome complex. The experiment was carried out by using a solution of RSC containing $160 \mu\text{g}$ protein/ml in a buffer containing 50 mM potassium acetate, 3 mM magnesium chloride, and 15 mM HEPES, pH 7.5. The nucleosome samples were prepared using a solution

TABLE I
THE NUMBER OF PARTICLES IN AN ARBITRARY AREA IS LISTED FOR RSC (FIRST COLUMN),
NUCLEOSOMES (SECOND COLUMN), RSC IN THE RSC/NUCLEOSOME SAMPLES (THIRD
COLUMN), AND NUCLEOSOMES IN THE RSC/NUCLEOSOME SAMPLES. THE LAST ROW
SHOWS THE AVERAGE OF THE VALUES FOR EACH COLUMN^a

RSC	Nucleosomes	RSC/nucleosomes (RSC count)	RSC/nucleosomes (nucleosome count)
72	70	35	18
65	55	43	21
67	73	41	17
67	57	28	19
72	71	35	27
69	65	36	20

^a Analysis of these numbers indicates that there is an overall decrease in the number of particles per unit area after mixing of RSC and nucleosomes, probably as a result of mutual charge neutralization that decreases the affinity of the particles for the amorphous carbon film support. It also reveals a 40–50% decrease in the expected number of nucleosomes in the RSC/nucleosome particles, suggesting that about half of the RSC particles have a bound nucleosome.

with a concentration of 50 $\mu\text{g/ml}$ in the same buffer. Formation of the RSC/nucleosome complex was carried out by mixing RSC and nucleosome solutions resulting in the same final concentration of both components as used for preparation of single-component samples, and incubating the resulting mix for 30 min at $\sim 30^\circ$. The results, summarized in Table I, indicate that the number of free nucleosomes diminished by about 40–50% when the nucleosomes were incubated with RSC. The conclusion from this analysis is that the RSC/nucleosome complex seems to be at least partially stable under the acidic conditions ($\text{pH} \sim 4$) of the uranyl acetate solution used to preserve the particles.

To further evaluate formation of the RSC/nucleosome complex, images of particles selected from the RSC/nucleosome samples were aligned and subject to statistical analysis as described before. While a relatively large (~ 12) number of distinguishable conformations were detected in RSC samples (see Fig. 1), variability in the structure of RSC seems to be significantly reduced in the presence of nucleosomes. As shown in Fig. 3, only four distinct conformations of RSC were detected when nucleosomes were present. The decrease in the number of free nucleosomes in the presence of RSC, and the clear stabilization of the RSC conformation in the presence of nucleosomes, point to the stability of the RSC/nucleosome complex under the conditions of our EM analysis. A reconstruction calculated from the largest set of RSC/nucleosome images is shown in Fig. 4.

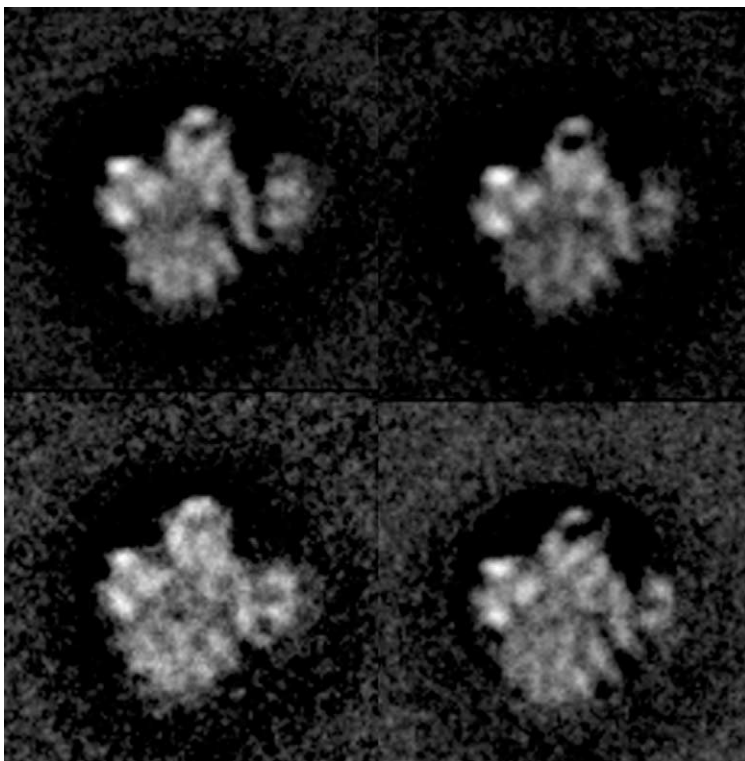


FIG. 3. Structure of the RSC/nucleosome complex in projection. The RSC/nucleosome complex was formed by incubating RSC and nucleosomes in a buffer containing 50 mM potassium acetate, 3 mM magnesium chloride, and 15 mM HEPES, pH 7.5. A total of ~ 9260 images of particles preserved in uranyl acetate were computationally aligned and sorted into homogeneous classes using multivariate statistical analysis and hierarchical ascendant classification.³ As observed for RSC alone, most particles appeared to be in the same orientation. However, interaction with the nucleosome seems to stabilize the structure of the RSC complex, as evidenced by the much smaller number of homogeneous groups generated by statistical analysis.

Additional density is present in the central cavity, in agreement with our suggestion that the nucleosome might bind in that location. However, the amount of additional density observed is less than that expected on the basis of the molecular weight of the nucleosome core particle. Such discrepancy is most likely due to inclusion of unoccupied RSC particles in the RSC/nucleosome image data set, as indicated by the data summarized in [Table I](#). Statistical analysis of the untilted RSC/nucleosome images (where the central cavity is clearly visible and does not overlap significantly

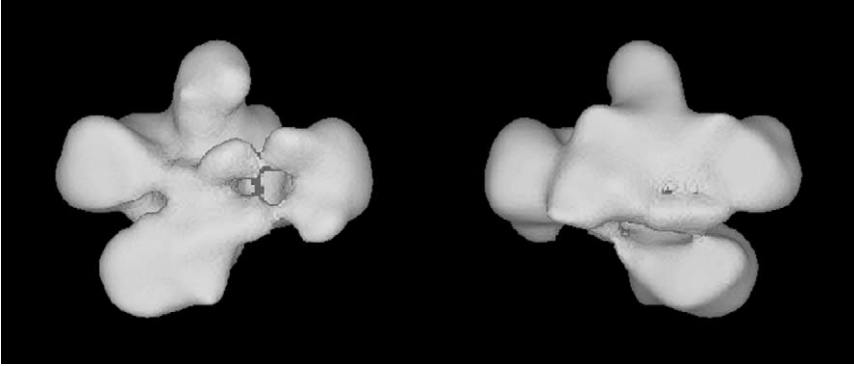


FIG. 4. Three-dimensional reconstruction of the RSC/nucleosome complex. The overall structure of the RSC complex remains constant after incubation with nucleosomes, but additional density is apparent in the central cavity. However, the additional density only corresponds to about half of that expected based on the molecular weight of the nucleosome core particle. Partial detection of the nucleosome is most likely due to the presence of unoccupied RSC particles in the data set, and to problems with staining caused by charged surfaces in the nucleosome and the RSC central cavity.

with the surrounding density that defines it) corresponding to the tilted particle images used to calculate the RSC/nucleosome reconstruction was carried out to attempt to separate empty and occupied RSC particles. The results from such analysis (not shown) were inconclusive, perhaps because the area corresponding to the central cavity includes only a relatively small number of pixels. Incomplete formation of the RSC/nucleosome complex detected by the particle count study (Table I), along with staining artifacts produced by the highly charged nature of the histone core and DNA surfaces, must contribute to the detection of an artificially low density in the central RSC cavity.

The structure of the RSC/nucleosome complex strongly suggests that interaction of a nucleosome with RSC occurs by binding of the nucleosome to the central cavity in the RSC complex. The size and shape of the central cavity match closely the size and shape of a nucleosome core particle. This is illustrated in Fig. 5, which shows our proposed model for RSC/nucleosome interaction. The RSC complex is shown in its prevalent conformation, and a low-resolution (~ 25 Å) structure of the nucleosome core particle (obtained by low-pass filtering of the atomic-resolution X-ray structure of the complex⁹) has been placed in the central RSC cavity.

⁹ K. Luger, A. W. Mader, R. K. Richmond, D. F. Sargent, and T. J. Richmond, *Nature* **389**, 251 (1997).

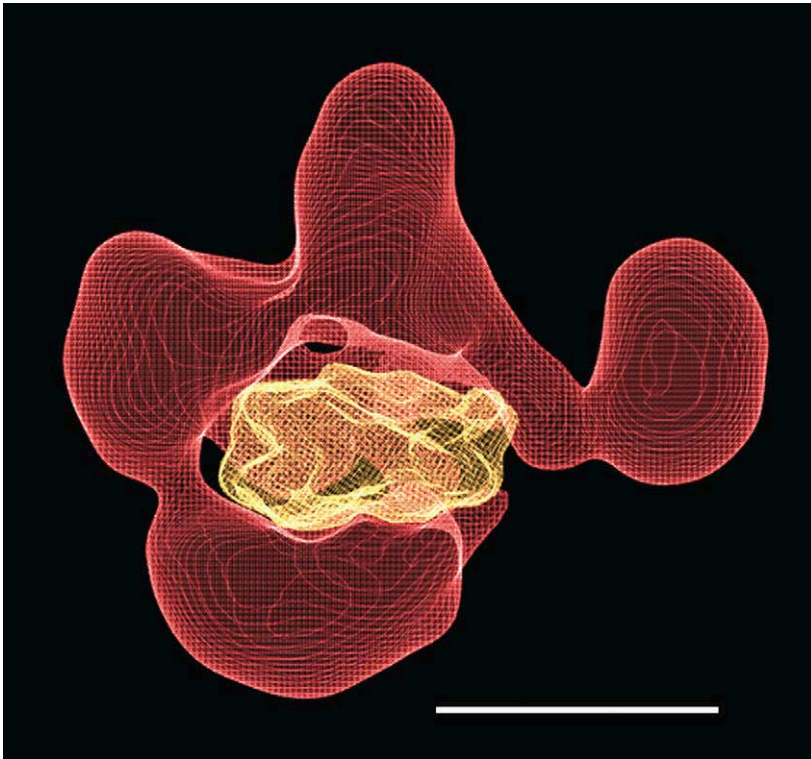


FIG. 5. Possible mode of RSC-nucleosome interaction. An X-ray structure of the nucleosome⁹ was filtered to 25 Å and manually fitted in the central cavity of the RSC structure [using the program O (T. A. Jones, J. Y. Zou, S. W. Cowan, and M. Kjeldgaard, *Acta Crystallogr. A* **47** (Pt 2), 110 (1991)).]. The close fit between the nucleosome and the RSC cavity is apparent. The scale bar corresponds to approximately 100 Å.

The figure illustrates the close fit of the nucleosome in the cavity. The model shown in Fig. 5 is supported by results from nuclease digestion studies of nucleosomal DNA in an RSC nucleosome complex, which indicate that digestion of nucleosomal DNA occurs preferentially at positions that would be more exposed in the model.⁴

Examination of Unstained RSC and RSC/Nucleosome Particles

While preservation of single particles in a heavy metal stain provides a simple and convenient way of obtaining structural information about a macromolecular complex, the results suffer from limitations in resolution and in the fidelity of the resulting volumes. These problems can be avoided

by examining unstained particles preserved in amorphous ice (cryo-electron microscopy), which makes possible direct imaging of molecular features, and has been shown to preserve molecular structure to near atomic resolution.¹⁰⁻¹² Preparation of frozen-hydrated samples has been extensively described¹³ and will not be repeated here. Instead, some of the issues encountered in applying the technique to the study of the RSC complex will be presented.

The first factor to consider is the type of grids to be used for sample preparation. Unstained particles can be adsorbed to a thin amorphous carbon support film, as in the case of stained samples. In fact, some of the highest resolution structures obtained by single particle analysis methods have actually been calculated from images of particles adsorbed to a support film.¹⁴ The presence of a support film also makes it possible to determine more accurately the defocus value of the images, a parameter that is critical for calculation of a meaningful reconstruction.¹⁵ Particles can also be preserved in a thin, unsupported film of amorphous ice, which is usually formed across holes in a relatively thick perforated carbon support film.¹⁶ Particles preserved in an unsupported amorphous ice film are not disturbed by interaction with a substrate, and there is no contribution to the background signal from a continuous support film. However, under those conditions particles are often found to preferentially interact with the air/water interface, and this can interfere with their preservation. Also, sample preparation usually requires the use of a protein solution with a much higher (>10-fold higher) concentration, as the particles often tend to adsorb to the edges of the perforated carbon support.

Frozen-hydrated RSC samples were prepared using grids with a continuous carbon support film. The experiments were complicated by apparent interaction of the particles with the air/water interface, even in the presence of the support film. Nonetheless, a number of RSC images suitable for analysis were obtained. There are two main differences between images of RSC particles preserved in amorphous ice and those of RSC particles preserved in stain. First, the frozen-hydrates particles no longer show a preferred orientation on the substrate film. Second, the conformation of

¹⁰ A. Miyazawa, Y. Fujiyoshi, M. Stowell, and N. Unwin, *J. Mol. Biol.* **288**, 765 (1999).

¹¹ G. Ren, A. Cheng, V. Reddy, P. Melnyk, and A. K. Mitra, *J. Mol. Biol.* **301**, 369 (2000).

¹² B. Bottcher, S. A. Wynne, and R. A. Crowther, *Nature* **386**, 88 (1997).

¹³ J. Dubochet, M. Adrian, J. J. Chang, J. C. Homo, J. Lepault, A. W. McDowell, and P. Schultz, *Q. Rev. Biophys.* **21**, 129 (1988).

¹⁴ J. Frank, P. Penczek, R. K. Agrawal, R. A. Grassucci, and A. B. Heagle, *Methods Enzymol.* **317**, 276 (2000).

¹⁵ P. Penczek, M. Radermacher, and J. Frank, *Ultramicroscopy* **40**, 33 (1992).

¹⁶ P. Penczek, R. A. Grassucci, and J. Frank, *Ultramicroscopy* **53**, 251 (1994).

the particles appears essentially homogeneous (i.e., there is no variation in the position of the lower module of the RSC structure). Images of particles preserved in amorphous ice were classified into homogeneous groups by aligning them to a set of reference projections of the RSC 3D reconstruction calculated from images of particles preserved in stain. To eliminate any possible reference-related bias, reference-free alignment was used to examine the homogeneity and alignment of each one of the particle groups defined by the classification. A gallery of the resulting reference-bias-free averages is shown in Fig. 6. The final step in obtaining a reconstruction

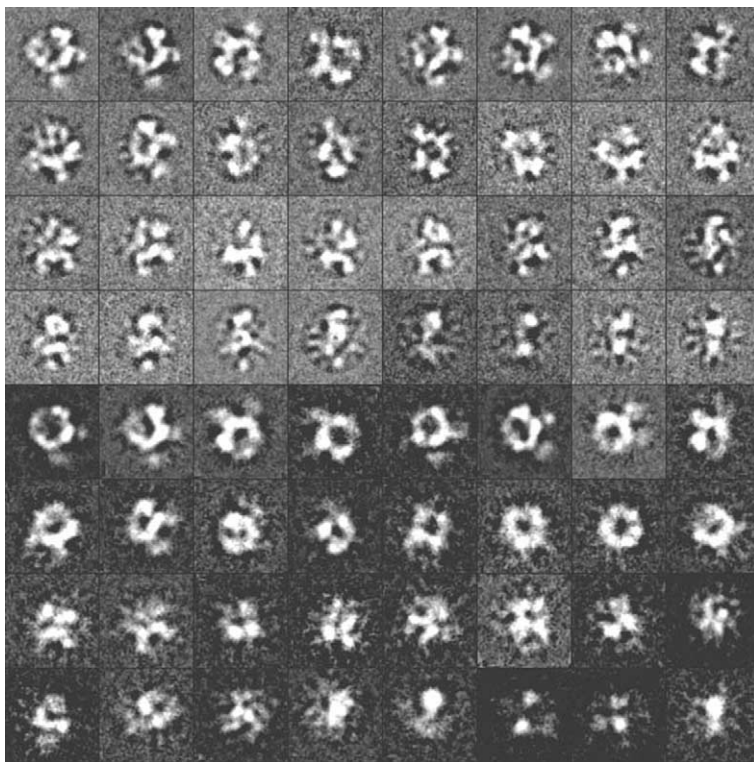


FIG. 6. Structure of unstained RSC in projection. Images of unstained, frozen-hydrated RSC particles were separated into groups based on their similarity to projections of the RSC reconstruction calculated from particles preserved in negative stain. The members of each homogeneous group were then realigned without use of a reference to avoid possible bias. Projections of the reference structure calculated from stained particles are shown in the four top rows. The corresponding group averages from unstained particles are shown in the bottom four rows. Improving the homogeneity of the groups, and determining the relative orientation of the resulting group averages, will make possible calculation of an improved RSC reconstruction.

of the RSC complex from the unstained particle images entails combining the information present in this set of projections. This requires precise knowledge of their relative orientations. Evidently, approximate information is provided by comparison with the available stain reconstruction. However, preliminary analysis indicates that the deformation induced by preservation in stain is significant, and this prevents direct use of the stain reconstruction as a meaningful reference for calculation of an improved reconstruction from the unstained particle images. We are currently working to obtain a suitable reference volume, which will allow us to make full use of the information contained in images of unstained RSC particles.

[5] Use of Optical Trapping Techniques to Study Single-Nucleosome Dynamics

By BRENT BROWER-TOLAND and MICHELLE D. WANG

Introduction

Over the past decade, optical trapping techniques have become a standard part of the repertoire of tools available for the study of biological molecules.¹⁻⁵ More recently, optical trapping techniques have been applied to the study of chromatin structure and even details of the structure of individual nucleosomes in a chromatin array.⁶⁻⁸

The general experimental design of optical trapping experiments with chromatin involves immobilization of one end of a linear DNA molecule on a surface, while the other end of the molecule is attached to a polystyrene microsphere (bead). The microsphere can then be used as a microscopic “handle” which can be captured and manipulated by the optical trap (Fig. 1). The optical trap can be used to exert and measure piconewton-scale

¹ K. Svoboda, C. F. Schmidt, B. J. Schnapp, and S. M. Block, *Nature* **21**, 365 (1993).

² H. Yin, M. D. Wang, K. Svoboda, R. Landick, J. Gelles, and S. M. Block, *Science* **270**, 1653 (1995).

³ M. D. Wang, M. J. Schnitzer, H. Yin, R. Landick, J. Gelles, and S. M. Block, *Science* **282**, 902 (1998).

⁴ J. Liphardt, B. Onoa, S. B. Smith, I. Tinoco, and C. Bustamante, *Science* **292**, 733 (2001).

⁵ S. J. Koch, A. Shundrovsky, B. C. Jantzen, and M. D. Wang, *Biophys. J.* **83**, 1098 (2002).

⁶ Y. Cui and C. Bustamante, *Proc. Natl. Acad. Sci. USA* **97**, 127 (2000).

⁷ M. L. Bennink, S. H. Leuba, G. H. Leno, J. Zlatanova, B. G. de Grooth, and J. Greve, *Nat. Struct. Biol.* **8**, 606 (2001).

⁸ B. Brower-Toland, R. C. Yeh, C. Smith, C. L. Peterson, J. T. Lis, and M. D. Wang, *Proc. Natl. Acad. Sci. USA* **99**, 1960 (2002).